ADVANCED LIFETIME SPECTROSCOPY –
DEFECT PARAMETERS OF IRON IN SILICON AND A NEW FINGERPRINT

S. Rein and S.W. Glunz

Fraunhofer Institute for Solar Energy Systems ISE, Heidenhofstr. 2, D-79110 Freiburg, Germany
Phone +49 761-4588-5271; Fax +49 761-4588-9250; Email: stefan.rein@ise.fraunhofer.de

ABSTRACT: As dissolved iron is one of the most common lifetime-killing contaminants in silicon, its coexisting defect configurations, interstitial iron (Fe$_i$) and iron-boron pairs (FeB), are investigated on an intentionally iron-contaminated silicon sample by means of temperature-dependent and injection-dependent lifetime spectroscopy (TDLS and IDLS). In good agreement with the literature, the study identifies the known Fe$_i$ donor level at E_t-$E_V = (0.394 \pm 0.005)$ eV and determines its symmetry factor as $k = \sigma_n/\sigma_p = 51 \pm 5$, which is an order of magnitude lower than expected from the literature. Using the well-confirmed k factor, the poorly-confirmed electron capture cross-section is re-determined as $\sigma_n = (3.6 \pm 0.4) \times 10^{-15}$ cm^2 at 300 K. The observed exponential $\sigma(T)$-dependence identifies the multiphonon emission mechanism as the dominant capture mechanism for electrons with an activation energy $E_\infty = 0.024$ eV. Moreover, the study reveals an additional fingerprint of iron which consists in a qualitative change of the TDLS curve upon illumination and its S-like shape under dark conditions. Based on this robust criterion, iron is identified as the limiting impurity in a standard industrial multicrystalline silicon sample.

Keywords: Lifetime, Spectroscopy, Defects, Iron.

1. INTRODUCTION

Dissolved iron is one of the most common lifetime-killing contaminants in silicon. In the case of boron doping it may be present as interstitial iron (Fe$_i$) or iron-boron pairs (FeB), which coexist at room temperature. The technological importance of iron arises on the one hand from the many sources of iron contamination during wafer processing and on the other hand from the detrimental effect both defect configurations have on the device performance even at very low concentrations. In spite of the intensive studies on iron in the past, there are still relevant defect parameters which are tainted with a high uncertainty [1, 2], as e.g. the symmetry factors $k := \sigma_n/\sigma_p$. To fill this gap, the present study aims at a complete characterization of especially the Fe$_i$ defect by analyzing an intentionally iron-contaminated monocrystalline p-type silicon sample by means of advanced lifetime spectroscopy. This technique, which is based on a combination of temperature-dependent (TDLS) and injection-dependent (IDLS) lifetime spectroscopy, has recently been developed and successfully been applied to characterize different impurities [3, 4]. Apart from giving new insight, the study is well suited to give further proof of the potential of lifetime spectroscopy as a diagnostic tool, as well-known Fe$_i$ parameters – such as the energy level E_t – will be confirmed. A detailed discussion of the theoretical background of the different lifetime spectroscopic techniques may be found in [5], including further details of the iron investigations presented here.

2. DEFECT TRANSFORMATION AND A NEW FINGERPRINT OF IRON IN SILICON

As the two defect configurations of iron (Fe$_i$ and FeB) are metastable, an investigation of their recombination properties requires a detailed knowledge of the defect transformation between the two states. It is well known from the literature [2] that dissociation of the FeB pairs may be induced thermally (at $T > 150°$C), optically or by minority carrier injection, while pair association requires the sample to relax in the dark at temperatures well below 100°C.

Investigating an intentionally iron-contaminated and boron-doped monocrystalline silicon sample with [Fe]=2.9×10^{12} cm^{-3} and [B$_s$]=2.9×10^{14} cm^{-3}, the impact of temperature and illumination on the injection- and temperature-dependent carrier lifetime has been studied carefully. To ensure an accurate determination of the bulk recombination properties, surface recombination is effectively suppressed by the use of a high-quality silicon-nitride surface passivation. Details about the experimental setup may be found in [5].

2.1 Fingerprint of iron in the Δn-dependence of carrier lifetime

Concerning the injection dependence of carrier lifetime at room temperature, our experiments (shown in [5]) confirmed the observations in the literature. While the FeB-dominated IDLS curve after sufficiently long dark storage exhibits a decreasing shape, the Fe$_i$-dominated IDLS curve after optical dissociation of the FeB pairs exhibits a steep increase. This qualitative change reflects a well-known characteristic of iron: while the Fe$_i$-defect exhibits the higher recombination activity under low-level injection (LLI), the FeB defect does so under high-level injection (HLI). Consequently, dissociation of FeB pairs leads to a lifetime decrease under LLI conditions and to a lifetime increase under HLI conditions. Recently Macdonald et al. suggested the crossover point of the two IDLS curves as a criterion to detect an iron contamination in silicon [6].

2.2 Fingerprint of iron in the T-dependence of carrier lifetime

Concerning the temperature dependence of carrier lifetime under LLI conditions, the impact of light soaking and temperature is displayed in Fig. 1. If the sample is kept in the dark before and in-between the lifetime measurements, the TDLS curve (open circles) exhibits an unusual S-like shape during ramping-up ①, which is reproduced during ramping-down ② if the sample is still kept in the dark. The unusual lifetime decrease between 95 and 155°C may be attributed to thermal dissociation ① (thermal re-association ②) of FeB pairs, as an increasing portion of Fe$_i$ reduces the effective carrier lifetime due to the higher recombination activity of the Fe$_i$ defect under LLI conditions (see above).
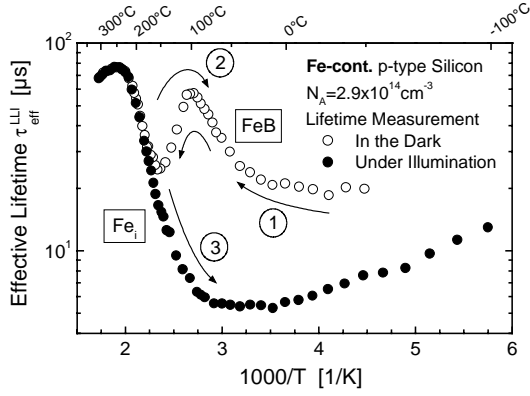
Fig. 1 Effect of light soaking and temperature on the temperature-dependent carrier lifetime under low-level injection measured by means of the MW-PCD technique on an iron-contaminated boron-doped Cz silicon sample ([Fe]=2.9×10^{12} cm^{-3}, [B$_s$]=2.9×10^{14} cm^{-3}). The S-like shape of the dark TDLS curve (*open symbols*), which results from thermal dissociation ① (thermal re-association ②) of FeB pairs, and the qualitative change of the TDLS curve upon illumination (*closed symbols*), which reflects an optically induced dominance of the Fe$_i$ defect in the whole T range, represent a robust fingerprint to detect iron in silicon.

This interpretation is strongly supported by the fact that the S-shape completely disappears if the ramping-down is not performed in the dark but under strong illumination (I_{bias}=0.3 W/cm^2) in-between the lifetime measurements (closed circles). If the dissociation of FeB pairs is stimulated optically, their thermal re-association below 155°C can obviously be avoided. It can be concluded that TDLS curve ③ (closed symbols) is dominated by the Fe$_i$ defect in the whole T range. The coincidence of the TDLS curves ① and ③ above 155°C proves a dominance of the Fe$_i$ defect in that temperature region even under dark conditions.

The above interpretation of the S-like TDLS shape is confirmed by the quantitative analysis in Fig. 2. In its lower half the temperature dependence of the equilibrium portions of FeB pairs (solid line) and Fe$_i$ ions (dashed line) is shown. It has been determined from the following empirical relation [7], the low doping concentration N_A of the investigated sample being taken into account:

$$\frac{[FeB]}{[Fe_i]} = C_1 N_A \times \exp\left(\frac{U_1}{k_B T}\right) \qquad (1)$$

with C_1=10^{-23} cm^{-3} and U_1=0.65 eV.

Since the equilibrium portion of Fe$_i$ increases in the T range from 95°C (TDLS peak) to 155°C (TDLS valley) from 33 % to 90 % and since the Fe$_i$ ion is the center of higher recombination activity under LLI conditions, the lifetime decrease observed above 95°C (open stars) is definitely due to thermal dissociation of FeB pairs. Since the equilibrium portion of Fe$_i$ exceeds 90 % above 155°C, the high-temperature part of the dark TDLS curve (open triangles) definitely reflects the recombination properties of the Fe$_i$ defect. Unfortunately, thermal dissociation not only influences the high-temperature part of the dark TDLS curve. As the equilibrium portion of Fe$_i$ continuously increases from negligible 0.5 % at 25°C to 33 % at 95°C (TDLS peak), it becomes evident that the Arrhenius increase of the FeB-dominated part of the dark TDLS curve (gray circles) is significantly affected by thermal dissociation, which impedes an accurate TDLS analysis of the FeB defect.
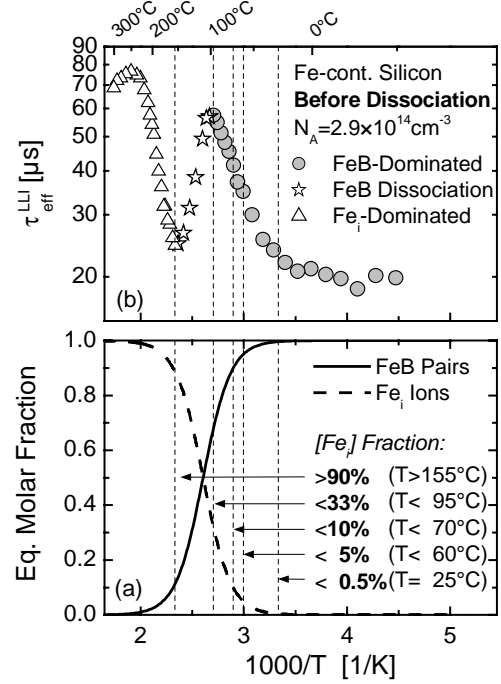
Fig. 2 (**a**) Equilibrium portions of FeB pairs (*solid line*) and Fe$_i$ ions (*dashed line*) as a function of temperature, only taking into account thermal dissociation. The calculations are based on the empirical Eq. (1) considering the low doping concentration of the sample under investigation. (**b**) Impact of the thermal dissociation of FeB pairs on the dark TDLS curve (① in Fig. 1). The *vertical lines* indicate different threshold values of the equilibrium [Fe$_i$] portion. Being negligible at room temperature, it increases up to 33 % at 95°C (TDLS peak).

While the S-like shape of the dark TDLS curves ①② has already been observed in two earlier TDLS studies [8, 9], the qualitative change of the TDLS curves upon illumination has not been reported so far. The qualitative change unambiguously disproves an interpretation of the S-shape given by Kaniava et al. [9]. They explained the peak around 100°C by superimposed temperature-dependent carrier trapping and attributed the Arrhenius increase in the high-temperature region to another deep level of the FeB pair, which is not correct (see Fig. 2). The practical importance of the S-shaped dark TDLS curve and the qualitative TDLS change observed upon illumination is that it represents an additional *fingerprint* of an iron contamination. As there is no other contaminant known to show such a behavior, measuring the temperature-dependent lifetime in the dark and under strong illumination provides a very robust criterion to detect iron in silicon (see Sect. 3).

2. LIFETIME SPECTROSCOPIC ANALYSIS: INTERSTITIAL IRON

As the illumination chosen here results in complete optical dissociation of FeB pairs [6], the spectroscopic analysis of the TDLS and IDLS curves measured after optical dissociation aims at complete characterization of the Fe$_i$ defect. As far as we know, this has not yet been done by means of lifetime spectroscopy.

2.1 Advanced TDLS analysis

Fig. 3a displays TDLS curve ③, which reflects the recombination properties of the Fe$_i$ defect in the whole T range
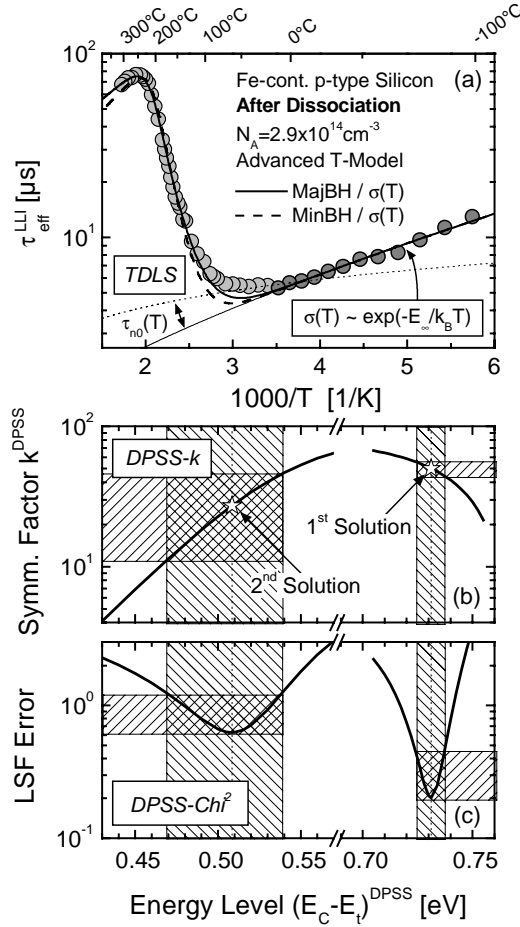
Fig. 3 Advanced SRH analysis of the Fe$_i$-dominated TDLS curve ③ by means of the defect parameter solution surface (DPSS) [4]. While an accurate modeling below 285 K (*dark gray circles*) requires the insertion of an exponential $\sigma(T)$-model (*thin solid line*), an accurate modeling of the TDLS bend due to intrinsic conduction (above 500 K) necessitates the advanced T-model. Taking into account both, the underlying $\sigma(T)$-model and the advanced T-model, the SRH modeling is performed for a MinBH (*dashed line*) and a MajBH defect (*solid line*). As the minimum values of the DPSS-Chi^2 curve differ significantly, the Fe$_i$-related defect level is unambiguously localized in the lower band gap half.

from 175 to 580 K. As a starting point of the spectroscopic analysis let us first determine the optimum configuration of the SRH model. As can be seen in Fig. 3a, the high-temperature part of the TDLS curve ($T>500$ K) is well described if the SRH model is based on the advanced T-model [4, 5], which takes into account the temperature dependence of both, the equilibrium carrier concentrations $n_0(T)$ and $p_0(T)$ and the band gap $E_{gap}(T)$ (for details see [5]). Concerning the low-temperature part ($T<285$ K), an accurate SRH modeling fails for $\sigma=$const (thin dotted line) and requires the introduction of a temperature-dependent capture cross-section. The fact that the measured TDLS data equal the minority capture time constant $\tau_{n0}(T)=[N_t v_{th}(T)\sigma_n(T)]^{-1}$ in the T range from 175 to 285 K (dark gray circles) allows an accurate determination of the underlying $\sigma(T)$-model. The observed $\tau_{n0}(T)$-decrease reflects an exponential increase of the capture cross-section with temperature, which can be modeled in terms of $\sigma(T)=\sigma_0\times\exp(-E_\infty/k_BT)$. Fitting this exponential $\sigma(T)$-model to the data (thin solid line), the

activation energy of the capture process is determined as $E_\infty=0.024$ eV. The identified $\sigma(T)$-model shows that carrier capture into the Fe$_i$ defect occurs via the multiphonon emission mechanism [5, 10].

Using the optimum configuration of the SRH model, which takes into account both, the underlying $\sigma(T)$-model and the advanced T-model, the SRH modeling of the TDLS curve is performed for a defect in the upper (MinBH defect, dashed line) and the lower (MajBH defect, solid line) band gap half as displayed in Fig. 3a. To enable a transparent spectroscopic evaluation of the TDLS curve, Fig. 3b and c display the associated defect parameter solution surface. This evaluation procedure has been introduced in Ref. [3, 4] and is discussed in detail in Ref. [5]. Since the DPSS-Chi^2 minimum in the MajBH is reduced by more than a factor three compared to the DPSS-Chi^2 minimum in the MinBH, the MajBH solution can be identified as the true solution. TDLS alone thus allows a complete characterization of the Fe$_i$-related defect level, which is localized in the lower band gap half at $E_t-E_V=(0.394\pm0.005)$ eV and found to exhibit a capture asymmetry of $k=51\pm5$. The errors of the extracted defect parameters are estimated from the DPSS diagram tolerating a least-squares error of twice its optimum value (shaded areas in Fig. 3b and c). As can be seen, both parameters of the MajBH solution are determined with high precision. While the E_t-precision is characteristic of any MajBH solution [4], the precision in the k-determination directly results from modeling the distinctive TDLS bend due to intrinsic conduction, which has been measured in a broad T range from 500 to 580 K. As demonstrated in [5] an accurate modeling of both the low- and high-temperature part of the TDLS curve is mandatory to obtain an accurate spectroscopic result.

2.2 Comparison of the LS result with the literature and discussion

The fact that the room-temperature IDLS curve (not shown) can be simulated precisely with the defect parameters determined from TDLS (see [5]) demonstrates the quality and reliability of the spectroscopic result. Lifetime spectroscopy thus identifies the Fe$_i$ donor level as the recombination-active defect level. While the E_t value is in excellent agreement with the average value of $E_t-E_V=(0.385\pm0.010)$ eV reported in the literature [1], the capture asymmetry of the Fe$_i$ donor level is found to be an order of magnitude lower than determined from the capture cross-sections published in the literature [2]. In spite of this strong deviation, the LS result is believed to be more reliable than the DLTS-based result from the literature. From a general point of view this is due to the fact that lifetime spectroscopy sensitively depends on k and thus allows a direct access, while DLTS only allows an indirect access via the capture cross-sections and faces the problem that the σ-determination is tainted with a relatively large uncertainty. Apart from these theoretical aspects, the LS result has to be favored in terms of experimental reproducibility. While the measured k value has been precisely reproduced by two independent LS techniques – TDLS and the combination of TDLS and IDLS –, the calculated k value had to be based on σ_n-results from the literature which are poorly confirmed and therefore uncertain. The symmetry factor k thus being well determined from LS

but significantly changed compared to the literature, recalculating the electron capture cross-section σ_n to remove the existing uncertainty suggests itself. Using for the hole capture cross-section the well confirmed average value of $\sigma_p = 7.0 \times 10^{-17}\,\text{cm}^2$ (at 300 K) [2] and calculating the product $\sigma_n = k \times \sigma_p$, we find for the electron capture cross-section of the Fe_i donor level a value of $\sigma_n = (3.6 \pm 0.4) \times 10^{-15}\,\text{cm}^2$ (at 300 K). Apart from the results presented here, it is shown in [5] that spectroscopic evaluation of the FeB-dominated TDLS and IDLS curves allows the FeB defect to be characterized.

3. IDENTIFICATION OF IRON IN MULTI-CRYSTALLINE SILICON

To demonstrate the practical use of the iron fingerprint proposed above, standard industrial multicrystalline silicon (as-cut) has been investigated by means of TDLS. Fig. 4 displays the dark TDLS curve of the mc-Si sample (lower half) in comparison with that of the iron-contaminated monocrystalline Cz-Si sample (upper half, see Fig. 2). As can be seen, the TDLS curve of the mc-Si sample exhibits the same qualitative structure as the reference sample. The fact that the characteristic local maximum and minimum are observed at the same equilibrium fractions of Fe_i (dashed vertical lines, calculated with Eq. (1)) and that the Fe_i-dominated Arrhenius increase (triangles) shows the same slope, clearly identifies iron as the limiting impurity in the mc-Si sample. The observed shift of the S-like TDLS structure towards higher temperatures and its less distinctive shaping directly result from the much higher doping concentration of the mc-Si sample (see Eq. (1)). For samples with industrially relevant doping concentrations above $10^{16}\,\text{cm}^{-3}$, the study thus reveals the iron-specific TDLS characteristics to be observed at temperatures above 170°C and 250°C, respectively. This underlines the importance of the accessible temperature range and defines a basic requirement for future TDLS measuring setups, as iron is one of the most important impurities. Moreover, it is expected that an SRH modeling of the entire TDLS curve with the defect transformation being taken into account allows the iron defect concentration to be determined accurately.

4. CONCLUSION

The study reveals a new fingerprint of iron in silicon consisting in a qualitative change of the TDLS curve upon illumination and an S-like shape of the TDLS curve measured in the dark. Not being reported for any other contaminant, these characteristics represent a very robust criterion to unambiguously identify iron in silicon as demonstrated here on industrial multi-crystalline silicon. The study on an intentionally iron-contaminated monocrystalline sample allows a complete characterization of the Fe_i donor level and provides new and deeper insight into its recombination properties. While its energy level is confirmed at $E_t\text{-}E_V = (0.394 \pm 0.005)\,\text{eV}$, its symmetry factor is determined as $k = \sigma_n / \sigma_p = 51 \pm 5$, which is an order of magnitude lower than expected from the literature and allows the poorly confirmed electron capture cross-section to be recalculated as $\sigma_n = (3.6 \pm 0.4) \times 10^{-15}\,\text{cm}^2$ at 300 K. The consistency of the spectroscopic results obtained from different LS techniques and the very good agreement of the E_t results obtained from LS (present study) and DLTS (literature), further prove the
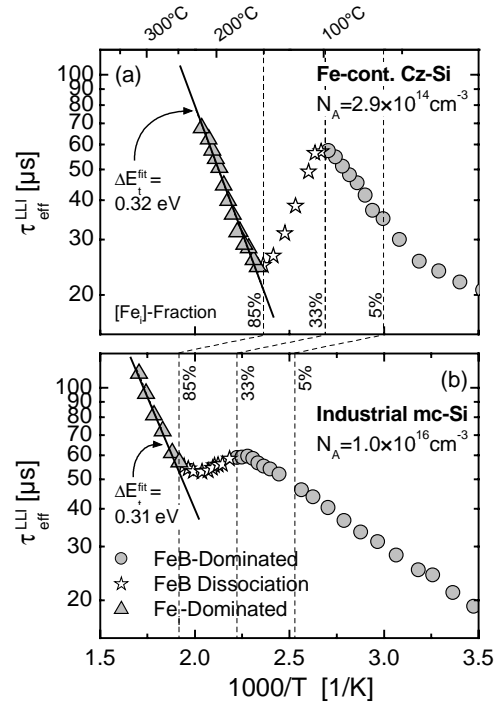
Fig. 4 Iron detection by means of the S-like shape of the dark TDLS curve (fingerprint): (**a**) intentionally iron-contaminated Cz-Si sample (① in Fig. 1) shown as reference; (**b**) industrial multi-crystalline silicon sample. The TDLS curve of the mc-Si sample exhibits the same qualitative structure as that of the reference sample with the local maximum and minimum being observed at the same equilibrium fractions of Fe_i (*dashed vertical lines*) and with the Fe_i-dominated Arrhenius increase (*triangles*) showing the same slope. This identifies iron as the limiting impurity in the mc-Si sample.

excellent performance of lifetime spectroscopy. As the most sensitive technique [11] to detect and determine an iron contamination in silicon heavily relies on the Fe_i and FeB defect parameters [6], the spectroscopic results are of special practical importance (see [5]).

REFERENCES

[1] K. Graff, *Metal Impurities in Silicon-Device Fabrication*, 2nd ed. (Springer, Berlin-Heidelberg, 2000).

[2] A.A. Istratov, H. Hieslmair, and E.R. Weber, Appl. Phys. A **A69** (1), 13-44 (1999).

[3] S. Rein and S.W. Glunz, Appl. Phys. Lett. **82** (7), 1054-56 (2003).

[4] S. Rein and S.W. Glunz, *Proc. 19th EU-PVSEC* (Paris, France, 2004), p. 479-83.

[5] S. Rein, *Lifetime Spectroscopy – A Method of Defect Characterization in Silicon for Photovoltaic Applications,* in: Springer Series in Materials Science (Springer, Berlin-Heidelberg, 2005).

[6] D.H. Macdonald, L.J. Geerligs, and A. Azzizi, J. Appl. Phys. **95** (3), 1021- 8 (2004).

[7] L.C. Kimerling and J.L. Benton, Physica **116B+C**, 297-300 (1983).

[8] Y. Hayamizu, T. Hamaguchi, S. Ushio, T. Abe, et al., J. Appl. Phys. **69** (5), 3077-81 (1991).

[9] A. Kaniava, A.L.P. Rotondaro, J. Vanhellemont, U. Menczigar, et al., Appl. Phys. Lett. **67** (26), 3930-2 (1995).

[10] C.H. Henry and D.V. Lang, Physical Review B (Solid State) **15** (2), 989-1016 (1977).

[11] W. Bergholz, G. Zoth, G. Götz, and A. Saliov, Solid State Phenomena **19 & 20**, 109-20 (1991).